Evolution of a novel orally bioavailable series of PI3Kδ inhibitors from an inhaled lead for the treatment of respiratory disease.

[†]Augustin Amour, [†]Nick Barton, [†]Anthony W.J. Cooper, [†]Graham Inglis, [‡]Craig Jamieson, [†]Christopher N. Luscombe, Josie Morrell, [†]Simon Peace*, [†a]David Perez, [†]Paul Rowland, [†]Chris Tame, [†]Sorif Uddin, [†]Giovanni Vitulli and [†]Natalie Wellaway

[†]GlaxoSmithKline R&D, Gunnels Wood Road, Stevenage, SG1 2NY, U.K.

[‡]Department of Pure and Applied Chemistry, University of Strathclyde, 295 Cathedral Street Glasgow, G1 1XL, U.K.

Abtsract

A four step process of high quality modelling of existing data, deconstruction, identification of replacement cores and an innovative synthetic re-growth strategy led to the rapid discovery of a novel oral series of PI3Kδ inhibitors with promising selectivity and excellent *in vivo* characteristics.

Introduction

The phosphoinositide-3-kinases (PI3Ks) are a family of lipid kinases that are implicated in the development of a range of diseases, including respiratory inflammation.[1,2] They comprise three classes based on structure, mode of regulation and phospholipid substrate. The class I targets have been extensively investigated due to their role in various cancers and inflammatory disease,[3] with their biochemical role mediating the phosphorylation of phosphatidylinositol (4,5)-diphosphate (PtdIns(4,5)P_2), to produce phosphatidylinositol (3,4,5)-triphosphate (PtdIns(3,4,5)P_3).[4] A number of studies have highlighted the correlation between PI3K-mediated PIP3 production and T cell cytokine release[5], mast cell degranulation,[6] neutrophil chemotaxis,[7] and the production of reactive oxygen species.[8] These cell behaviours have been implicated in the development of respiratory inflammation and a range of cancers. Of the known isoforms, PI3Kδ is found to be predominantly expressed in leucocytes suggesting it is a promising target for the treatment of asthma,[9] COPD,[10] and autoimmune

disorders.[11] From a drug discovery perspective, selectivity among the isoforms is an important consideration; both PI3Kδ and γ knock-out mice are viable and display some impairments of immune cell functions,[12,13] however, PI3Kα and β knock-outs have been shown to be embryonically lethal.[12]

We recently reported the discovery of an inhaled clinical candidate GSK2292767 (**1**, Figure 1) as a potent and selective PI3Kδ inhibitor with promising *in vivo* properties as a potential therapy for respiratory indications[14]. This compound is structurally related to GSK2269557, also an inhaled therapy and currently in Phase II trials for COPD and asthma. Orally bioavailable compounds such as IPI-145[15] and GS-1101 (CAL-101, Idelalisib)[16] have previously been reported and advanced through clinical studies for oncology indications. Compounds of a similar structural genus have also appeared more recently, for example UCB-5857 and TGR-1202. All derive from the same chemical series which generally possesses mixed PI3Kδ/γ inhibition and this lack of selectivity creates difficulties in delineating the role of either isoform in inflammatory disease. More recently still researchers from Amgen reported potent, selective and orally bioavailable PI3Kδ inhibitors for the treatment of inflammatory disorders (e.g. AM-8508, **2**)[17] and Novatis have progressed CDZ-173 into phase III trials for the treatment of activated PI3K delta syndrome. Taken together these events highlight the significant and continuing level of interest associated with this promising therapeutic target. In the current study, we disclose our early efforts towards the discovery of a series of PI3Kδ selective, orally bioavailable compounds exemplified by the dihydroisobenzofuran derivative **3** (Figure 1) derived from our existing inhaled asset **1** as a potential therapy for respiratory disorders. The aim of the study was to discover an alternative core with reduced clearance and increased bioavailability whilst retaining the potential to deliver the class-leading levels selectivity demonstrated by compounds such as **1**.

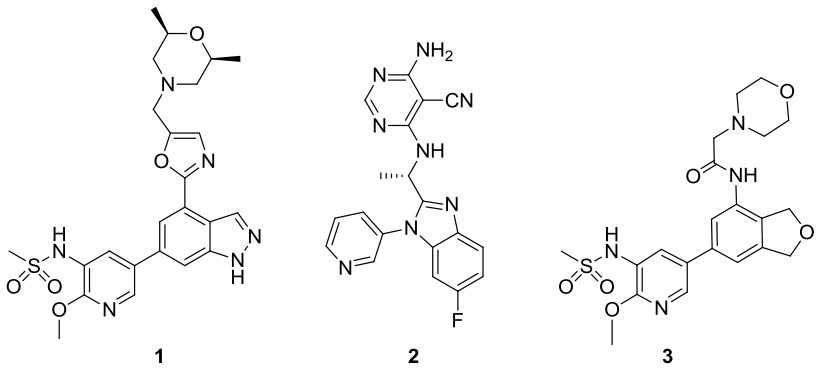

Figure 1. Structures of **1**, **2** and **3**.

Results and Discussion

Our progenitor compound **1** was developed for delivery by the inhaled route and exhibited negligible oral bioavailability (< 2%) with very low exposure (Cmax <2ng/mL, 3mg/kg p.o.) and only a small sub-set of the compounds prepared in this series possessed moderate bioavailability and clearance. With this in mind, we elected to pursue a four stage approach in order to evolve a series more suited to oral adsorption. 1) Utilise all available information to guide future approaches. 2) Deconstruct the current series to identify key features and provide an efficiency baseline. 3) Replace or remove perceived vulnerable moieties in the deconstructed molecules to provide a wide range of future options. 4) Select options with distinct risk profiles for re-growth/optimisation.

Step 1 – Utilisation of legacy information. Replacement of the indazole core was motivated in part by a desire to reduce the aromatic ring count[18] but primarily by contemporaneous literature reports that implicated the indazole group[19] as a target for time-dependent P450 inhibition. The general design strategy involved tuning of TPSA[20] (<135 $Å^2$) and limitation of molecular weight through consideration of ligand efficiency.[21] To further refine our approach two proprietary data-sets were inspected with a view to minimise oral dose. These were factors affecting clearance (*in vitro* and *in vivo*) and cellular potency/drop off. Whilst the clearance data presented no potentially transferable trends the data from the cell assays provided significantly more insight. The difference between the primary assay and cellular whole blood (bio phase) assay was calculated and this difference was modelled using a multivariate data analysis technique called Partial Least Squares regression,[22]

involving a standard set of physicochemical descriptors. The model was used to identify and explore potential relationships between molecular properties and the measured difference. The Loadings Plot (Figure 2) explores the relationship between variables themselves and also between response in question. An examination of the plot highlighted three clusters of variables which led to assessment of which parameters were important. The associated Coefficient Plot summarises the magnitude and direction of influence of each variable.

Three key trends emerged from the data: i) Variables 5-9 are calculations of lipophilicity and appeared to be associated with a detrimental effect on drop-off between enzyme and whole blood potency; ii) Variables 11 and 12 suggested that ionisation, in particular addition of a basic centre, was beneficial to minimizing the drop-off between enzyme and biofluid activity; iii) The group of variables 23, 24 and 25 related to increased hydrogen bond donor count were detrimental to whole cell activity. The impact of lipophilicity and basic centres was attributed primarily to modulation of protein binding for which optimisation was not a priority; however, the negative impact of hydrogen bond donors, but not acceptors, drew our attention and impacted on our subsequent design strategy (*vide infra*). It is interesting to note that PI3Kdelta potency (variable 2) positively correlates with cellular drop off, albeit with very high variability, and it is not unlikely that this observation results from a relationship between lipophilicity and potency.

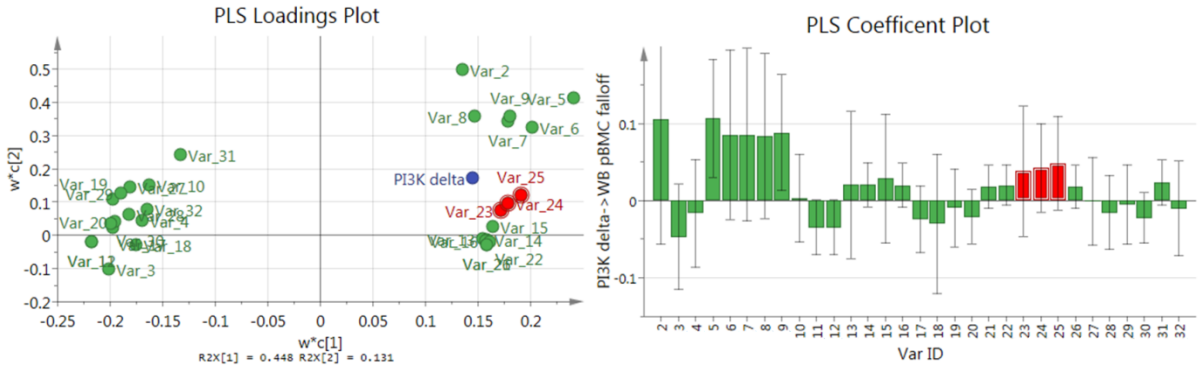

Figure 2 (a) PLS Loadings Plot demonstrating groups of coefficients (b) PLS Coefficient Plot indicating magnitude, direction and 95% confidence interval of the mean. Variables of interest: Var 5-8 (ACD Labs v11.logd at pH2, 5.5, 6.5 & 7.4) and Var 9 (clogP 481); Var 11 (positive ionisable

centre count) and Var 12 (total charge); Var 23 (estate.amideNH-sum), Var 24 (estate.amideNH-av) and Var 25 (estate.amideOtoNH-av). NB Var 2 is PI3K delta potency.

Step 2 – Deconstruction. A deconstruction (D_x, Figure 3) of compound 1 was performed to establish the minimum necessary pharmacophore and maximal potential efficiency of the lead series. It was anticipated that scanning for replacement components at a reduced complexity level would be considerably more synthetically tractable. Furthermore, scanning with fully-elaborated compounds runs the risk of small changes in optimal binding pose of the core preventing efficient binding of the entire molecule. For efficiency measurements we adopted Binding Efficiency Index[23] (BEI = 1000 x (pIC50/MW)) as our efficiency metric given that in our hands it proved to be intuitive to use yet correlates[24] very well with the more widely used Ligand Efficiency (LE). The deconstruction was conducted with some knowledge of the binding of the molecule[14] gleaned from homology modelling prior to the later generation of a crystal structure. The indazole core fragment (red) occupies the kinase 'hinge' region, the pyridyl sulfonamide (blue) entered the lipid-kinase 'back' pocket whilst the oxazole/morpholino group (magenta) occupied a vector that delivered majority of selectivity for PI3Kδ.

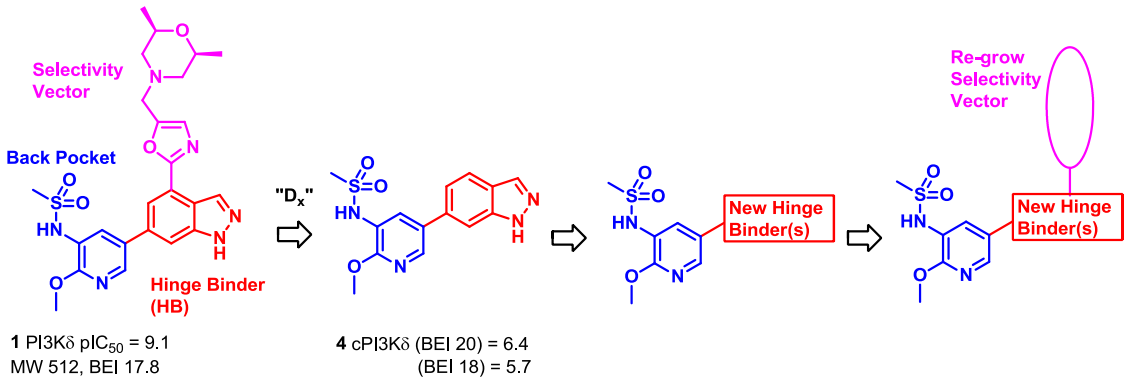

Figure 3. Design strategy for oral series. The calculated potency is derived *via* the rearranged BEI calculation (cPI3Kδ pIC_{50} = 320 x (BEI/1000))

The parent pyridine sulfonamide back-pocket binder (blue) was chosen as a structural lock. BEI calculations suggested that truncate **4** should be significantly above the limit of detection of the assay (pIC_{50} ~ 5) assuming a BEI of 18-20, hence allowing replacement hinge binding groups to be profiled.

Synthesis and evaluation of **4** (Table 1) confirmed the anticipated level of potency against PI3Kδ, validating its use as a benchmark for replacement groups.

Step 3 - Identification of replacement hinge-binding groups. A variety of potential hinge-binding groups were then scanned and one of the most promising hits from this exercise was the dihydroisobenzofuran analogue **5** (Table 1) as a potentially novel replacement. This moiety increased solubility which was perhaps surprising given the higher measured LogD of the compound. We reasoned that this may be the result of destabilisation of the solid form as a consequence of reduced planarity and elimination of inter-molecular hydrogen bonds. This observation, coupled with the previous analysis suggesting the benefit of reduced HBD count, encouraged us to re-institute the selectivity vector on this template to establish the potential for obtaining selectivity, whole blood efficacy and favourable DMPK parameters.

Table 1. Profile of reduced complexity analogue **4** and indazole replacement **5**.

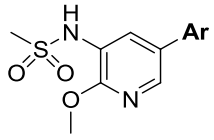

Ar	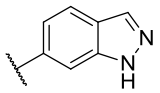	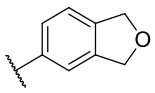	
	4	**5**	**1**
PI3Kδ pIC_{50} (n, BEI)	6.0 (4, 18.9)	6.1 (6, 19.0)	10.1* (2, 19.7)
PI3Kα,β,γ pIC_{50} (n)	5.1, 5.1, 5.6 (5)	5.4, 5.7, 5.5 (6)	6.3, 6.2, 6.3 (17+)
Chrom LogD pH 7.4	2.6	3.5	3.3
TPSA	97	78	135.5
Aryl Rings/HBD	3/2	2/1	4/2
Solubility (μg/mL)	31	92	182

*pKi[14]

Step 4 – Re-growth and optimisation. Having established the feasibility of replacing the indazole core, the subsequent phase of the optimisation trajectory focused on re-establishing the selectivity vector at the 6-position of the dihydroisobenzofuran template. The design hypothesis at this stage focused on generating compounds that would facilitate a thorough comparison with the indazole series and lead to an understanding of how well the SAR would transfer between the two series. To select the most appropriate functional groups for the 6-position, we considered the structures of PI3Kδ compounds previously synthesised in our laboratories, focusing on the key pyridylsulfonamide motif. The subset of compounds identified from this approach was further filtered through applying physicochemical property constraints that would be likely to furnish compounds with oral bioavailability. This analysis led to the identification of six potential substituents for inclusion at the 6-position of the dihydroisobenzofuran which spanned a variety of different chemotypes and offered a range of PI3K class I selectivity profiles. The substituents of interest are shown in Figure 4 as part of the dihydroisobenzofuran motif, with calculated physicochemical parameters shown in Table 2.

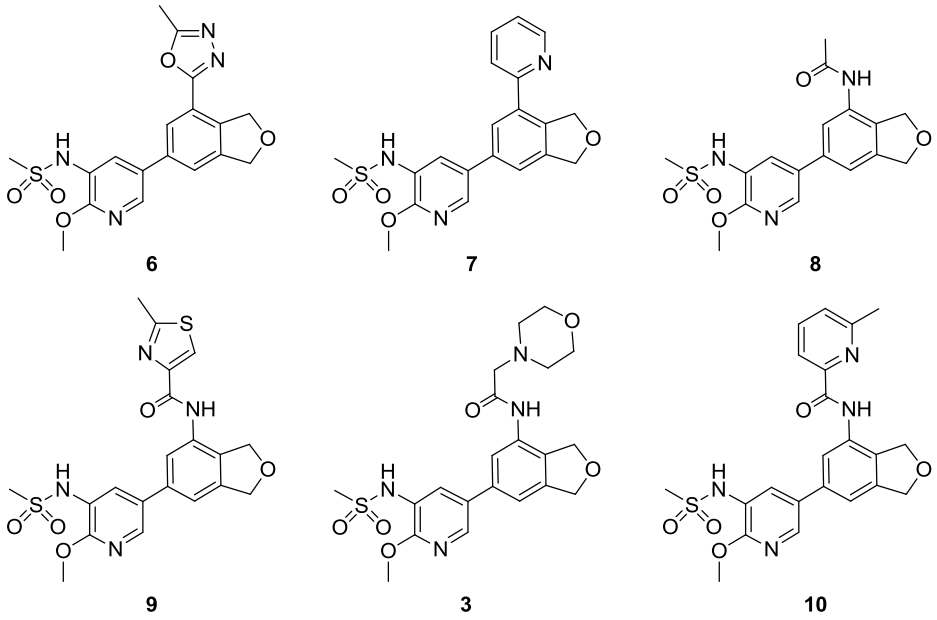

Figure 4. Target 6-position substituents in the dihydroisobenzofuran series.

The calculated physicochemical data is summarised in Table 2. In addition to reduced hydrogen bond donor count, target compounds had lower TPSA than the progenitor inhaled compound **1** and we anticipated that this could potentially translate into improved oral exposure.[20] Other aspects of the

physicochemical profile such as number of aromatic rings are lower, leading to potential improvements in Property Forecast Index (PFI), again increasing the probability of enhancing oral exposure.[18] The overall hydrogen bond donor count is included in the table; however, it is worth noting that all of the compounds contain one fewer donor than the corresponding progenitor indazoles.

Table 2. Calculated physicochemical properties for compounds **6** to **10**.

Phys. Chem. Property	**6**	**7**	**8**	**9**	**3**	**10**
MW	402	397	377	461	463	455
cLog P	1.1	2.9	1.5	2.8	2.9	1.6
TPSA	116	90	107	120	120	120
No. Ar rings	3	3	2	3	2	3
Rotatable bonds	4	4	4	5	6	5
Hydrodgen Bond Donors	1	1	2	2	2	2

Chemistry

Reduced complexity analogues **4** and **5** were prepared using a Suzuki-Miyaura coupling from the pinacol boronic ester **11**, Scheme 1.

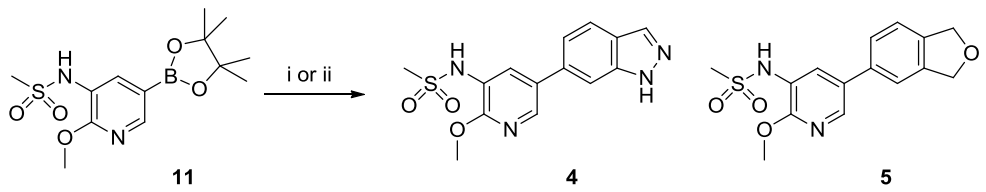

Scheme 1 Reagents and conditions (i) Boronate ester **11**, 6-bromo-1*H*-indazole, $Pd_2(dba)_3$, $^tBu_3P.HBF_4$, KF, 2-methylTHF/water (3:1), 28%. ii) Boronate ester, 5-bromo-1,3-dihydroisobenzofuran, $PdCl_2(dppf).DCM$, CsOAc, KF, THF/water (20:1), 39%.

The fully elaborated dihydroisobenzofuran core was accessed in an efficient manner utilising a ruthenium mediated cyclotrimerisation reaction as outlined in Scheme 2. The tethered [2+2+2] trimerisation of terminal alkynes preferentially installs the required *meta* arrangement of R_4 and R_6. Judicious selection of these groups allows excellent flexibility to the medicinal chemist and synthesis of a wide variety of targets in short order (4-6 steps). Literature reports[25] suggested that trimethylsilyl tethered diynes (R_6=TMS) exhibit excellent regiochemistry in this reaction and *ipso* substitution of the resulting aryl silane to iodide is well known (*vide infra*). It is worth noting that the route also provides the opportunity to make other changes to the core framework. For example use of nitriles (A=N) allows access to pyridyl analogues and elaboration at R_2 and R_7 readily facilitates substitution adjacent to the hinge-binding oxygen atom, therefore the investment was made in enabling this potentially challenging chemistry.

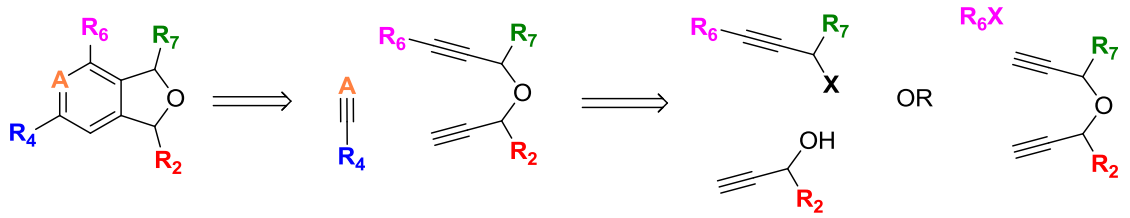

Scheme 2 Synthetic plan for the utilisation of 2+2+2 trimerisation chemistry.

Alkyne **13** was prepared as indicated in Scheme 3 and the TMS-protected bispropargylether **12** prepared in one step from propargyl ether according to the literature procedure.[26]

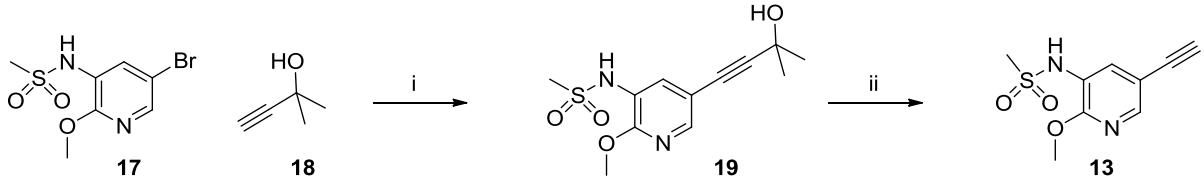

Scheme 3. (i) $Pd(PPh_3)_2Cl$ (8 mol%), CuI (8 mol%), Et_3N (4eq), 2-Me THF, 80 °C, quantitative; (ii) KOH, *i*PrOH, reflux, 77%.

The synthesis of the target compounds is described in Scheme 4. Optimisation of cyclotrimerisation conditions revealed that cyclopropylmethyl ether (CPME) was preferable to the commonly used dichoroethane as solvent.[27] The key aryl silane intermediate **14** was thus obtained in good yield with either a 1.2 eq excess of **12** or a 2.0 eq excess of **13**. *Ipso* substitution of **14** with iodine monochloride then provided the iodo derivative **15** in excellent yield. Palladium-mediated cross coupling provided **6** and **7** using either a Negishi protocol[28] or modified Suzuki-Miyaura procedure,[29] respectively. Copper mediated amination of **15** provided aniline **16** which was then converted to amides **3, 8, 9** and **10**.

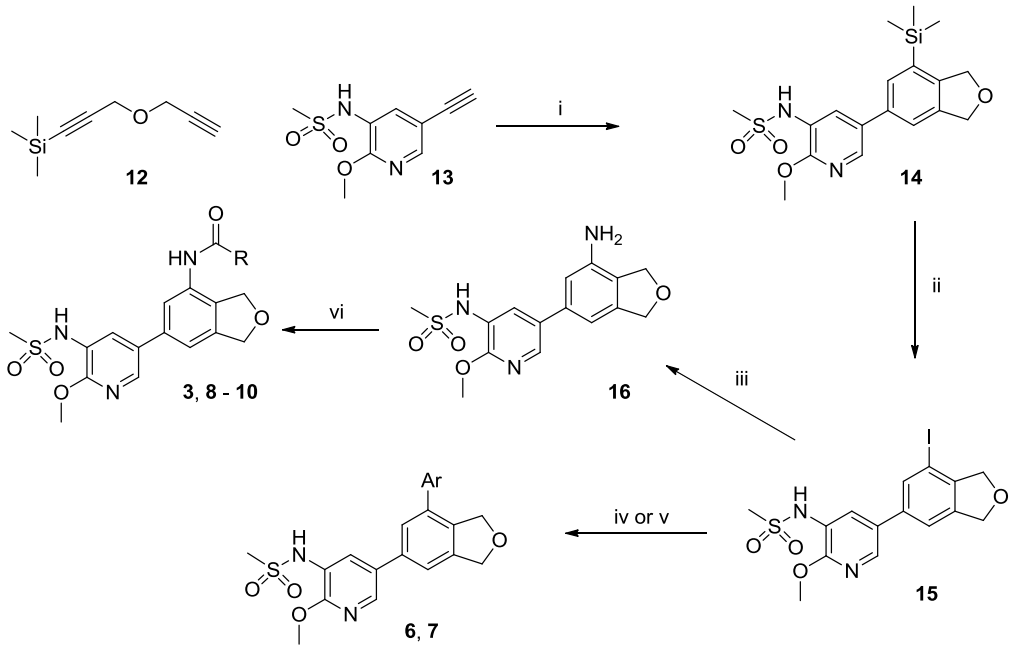

Scheme 4. (i) RuCp*(cod)Cl (10 mol%), CPME, r.t., 64% (1.2 eq **12** or 2.0eq **13**); (ii) ICl, CH_2Cl_2, 10 – 0 °C, 80%; (iii) CuI (20 mol %), L-Proline, Cs_2CO_3, DMSO:NH_3 (aq) (1:1), 110 °C, µwave, 77%; (iv) 2-(4,4,5,5-tetramethyl-1,3,2-dioxaborolan-2-yl)pyridine, $Pd(OAc)_2$ (1 mol %), Cs_2CO_3, dppf (20 mol %), CuCl (100 mol%), DMF, µwave, 100 °C, 10%; (v) (a) 2-methyl-1,3,4-oxadiazole, LiHMDS, $ZnCl_2$, THF, -10 °C; (b) $Pd(PPh_3)_4$ (10 mol%), Cs_2CO_3, µwave, 150 °C, 24%; (vi) RCO_2H, HATU, DMF, r.t., 21- 28%.

The *in vitro* potencies of the target compounds were measured in a homogenous time-resolved fluorescence assay as described previously.[14] The results from these assays (Table 4) indicate good levels of potency against the PI3Kδ isoform, with pIC_{50} values ranging from 6.4 to 8.3. The more structurally elaborated thiazole **9** and pyridine **10** display the most encouraging potency and selectivity profiles, providing support the original hypothesis that functionalisation at the 6-position of the dihydroisobenzofuran core would provide an enhancement of activity. In relation to PI3K class I selectivity, the majority of the analogues showed an encouraging profile in comparison to the progenitor dihydrosiobenzofuran **5**, particularly compounds **9**, **3** and **10**. In general the isoform selectivity observed was lower than the fully optimisied inhaled candidate molecule; however, comparison to the previously reported thiazole analogue **20** indicates similar selectivity is retained with the new hinge binder. Accordingly, we reasoned that selectivity could be improved by further optimisation of the 6-position vector**.**

Table 4. Isolated enzyme assay results for the PI3K class I isoforms.

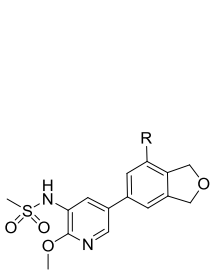

3, 5-10

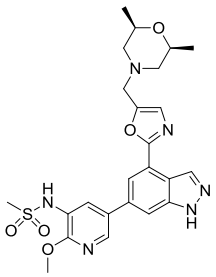

1

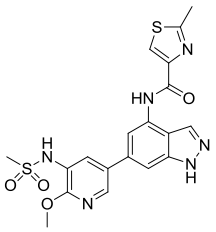

20

Compound Number	R	PI3K Class I isoforms			
		pIC_{50}	Selectivity vs PI3K δ (Ratio)		
		δ	α	β	γ
1	Inhaled PI3Kδ lead	10.1*	631	794	631
5	H	6.1	5	2.5	4
6	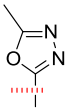	7.7	5	13	5
7	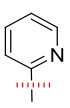	7.2	10	20	6

8		6.4	4	13	13
9	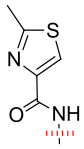	8.1	50	63	25
20	-	7.9	63	63	16
3	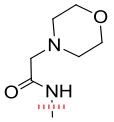	6.8	25	63	50
10	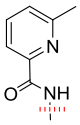	8.3	50	126	25

*pKi quoted[14]

Based on this promising initial data, and to more fully benchmark this nascent lead series, a selection of compounds was made for further profiling in both whole blood[14] to assess the cellular activity of each compound and DMPK[30] assays, as well as other developability screening. The results of these studies are summarised in **Table 5**.

Table 5. Further profiling of dihydroisobenzofuran analogues.

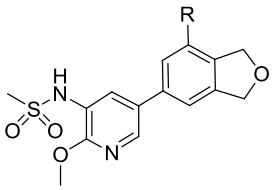

		R		
	Inhaled PI3Kδ lead	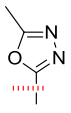	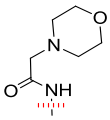	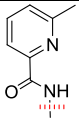
Compound number	**1**	**6**	**3**	**10**
PI3Kδ isolated enzyme (pIC_{50})	9.1	7.7	6.8	8.3
PI3Kδ whole blood (pIC_{50})	8.4	6.7	6.6	6.7
IVC rat, mouse, human liver microsomes (mL/min/g)	1.9, 5.9, 3.2	<0.5, 1.0, <0.5	<0.5, <0.5, <0.5	1.2, 1.4, <0.5
AUC_{inf}(p.o., ng.h/mL)	< 24	1370	673	42*

Half Life, $T_{½}$ (i.v.) (hr)	2.6	0.9	1.3	3.4
Cl (i.v.) (mL/min/Kg)	50.0	6.9	14	6.0
Oral Bioavailability, F (%)	< 2.0	56	54	1.5
V_{dss} (L/Kg)	3.5	0.5	1.1	1.6
HSA binding (%)	90	90	64	93
CLND Solubility (µg/mL)	182	195	185	50
MDCK passive perm. (nm/s)	213	803	122	758

In vivo PK data in Table 5 were obtained in the CD Sprague male rat following administration of 1mg/kg oral and *iv* doses. *AUC_{0-t} quoted.

Comparing the whole blood potencies for the newly synthesised compounds shows a drop off cellular activity of at least ten fold or greater for compounds **6** and **10**. By contrast, compound **3** exhibits only minimal attenuation in cellular potency compared to the isolated enzyme data. A likely contributor to this difference is protein binding given that compound **3** has an estimated free fraction of 36%, whereas the other analogues examined have an estimated free fraction of 10% or less. It is worth noting that whilst these compounds are substantially weaker than the inhaled lead in whole blood cell assays; however, there is a stronger imperative for potency for an inhaled molecule due to the necessity of a very low dose. The whole blood activity of **3**, **6** and **10** compare favourably with oral compounds in clinical development, for example the PI3Kδ/γ inhibitor IPI-145 inhibits basophil degranulaton with an IC_{50} of 96nM (pIC_{50}~7.0) in whole blood[15].

All three compounds display much improved metabolic stability when compared to the inhaled lead **1** in both *in vitro* and *in vivo* studies. *In vitro* clearance (IVC) levels in all species investigated are low to moderate, whilst rat *in vivo* clearance for compound **3** of less than 14 mL/min/Kg equates to less than 20% liver blood flow (Table 5). The slightly elevated observed clearance of morpholine **3** with respect to oxadiazole **6** and pyridine **10** could be attributed to the lower level of protein binding (HSA), which may increase the fraction of drug exposed to organs of metabolism and excretion. The relatively low volumes of distribution for compounds **6** and **3** result in lower half-lives compared to pyridine analogue **10**. It was reasoned that further optimisation of the 6-position (e.g. modulation of the basic amine) could increase volume of distribution and positively impact the half-life.

Low bioavailability is observed for pyridine **10** despite its low systemic clearance and excellent *in vitro* passive permeability measured on MDCK cells. First pass metabolism or poor absorption from the GI tract are therefore unlikely causes of the low bioavailability and it is more likely that this is attributed to the low solubility of pyridine **10** (50 μg/mL) when compared to the other dihydroisobenzofuran analogues examined. Oxadiazole **6** and morpholine **3** show significantly higher bioavailability than the inhaled lead **1**, thus validating the initial design hypothesis in controlling physicochemical properties. Furthermore, morpholine **3** is among a paucity of compounds from this chemotype which exhibit both oral bioavailability and greater than 20 fold PI3K class I selectivity in isolated enzyme assays. In addition to this, compound **3** also exhibited excellent selectivity against a varied panel of kinases and other enzymes.[31] Based on all of the above, we believe that the dihydroisobenzofuran series represents a significant advance in the design of selective PI3Kδ compounds which are suitable for oral administration.

Compound **3** was also successfully co-crystallised with PI3Kδ which confirmed the proposed binding mode with the kinase (**Figure 5**). From our earlier studies, the indazole was shown to be a hinge binding motif[14] and this interaction is effectively maintained by the dihydroisobenzofuran, albeit that any interaction between the indazole NH and the hinge has been lost. The 6-position substituent forms a similar vector to that observed with the inhaled lead **1**; however, the core benzenoid ring appears to be rotationally displaced by approximately 15 degrees which suggests that the optimal 6 position groups could differ between the two series. It is also worth noting that the morpholine substituent does not reach the same region of the protein as that occupied by **1** leading to the hypothesis that further selectivity can be obtained. Given the rotational displacement of the core it is postulated that complete re-optimisation of the linking group is required to allow the morpholine group to access the region occupied by **1.**

Figure 5. X-ray structure of compound **3** (cyan) co-crystallised with PI3Kδ and over-layed with a crystal structure of compound **1** (orange).

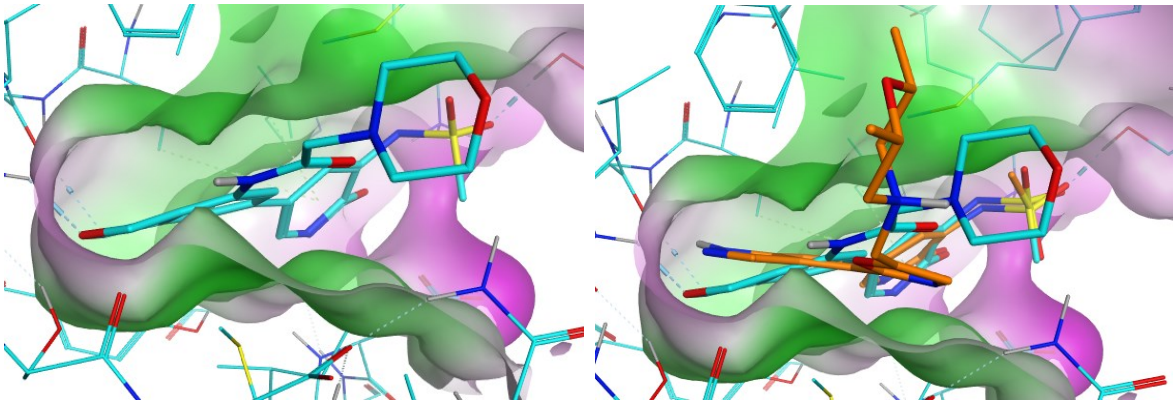

Based on its promising oral bioavailability and encouraging level of cellular potency the morpholine analogue **3** was progressed to an *in vivo* pharmacodynamic assay to determine its efficacy in a disease relevant animal model. In our previous report a Brown Norway rat acute OVA model of lung inflammation was used[14]. Compound **3** was assessed using this model whereby OVA challenge is administered 30 minutes after oral delivery. Significant protection against eosinophil recruitment was achieved by compound **3** at 3 mg/kg p.o (**Figure 6**) whereas failure to achieve significance at 9mg/kg is primarily attributed to two poorly responding rats in this group.

The pharmacokinetic data from the study is presented in **Table 6** along with the comparative data from the pilot pharmacokinetic study. Interestingly **3** achieved lower exposure in the OVA study at 3mg/kg when compared to the pilot study (1mg/kg) which may be result from strain dependency and/or differences in dose formulation. The blood concentration of **3** one hour after dosing, i.e. 30 minutes after OVA challenge, are 0.19uM and 1.27uM for the 3mg/kg and 9mg/kg groups respectively which compare very favourably with the pIC_{50} in human whole blood (6.6, 0.25uM, *vide supra*). The estimated free drug concentrations at this time-point are also provided.

From consideration of all the above data, morpholine **3** represents the inception of a promising series of PI3Kδ inhibitors with good oral bioavailability and robust levels of *in vivo* efficacy. This compares favourably to the benchmark set by the orally bioavailable dual PI3Kγ/δ dual inhibitor IPI-145, which demonstrates similar levels of *in vivo* efficacy in a related pharmacodynamic study and has recently completed a Phase 2a trial for asthma.

This highly encouraging data provides additional validation for the design strategy adopted in developing a new hinge binder, thereby providing confidence in further developing the dihydroisobenzofuran series to further optimise its selectivity and DMPK characteristics.

Figure 6. Pharmacodynamic Testing of compound **3** in an acute model of lung inflammation.

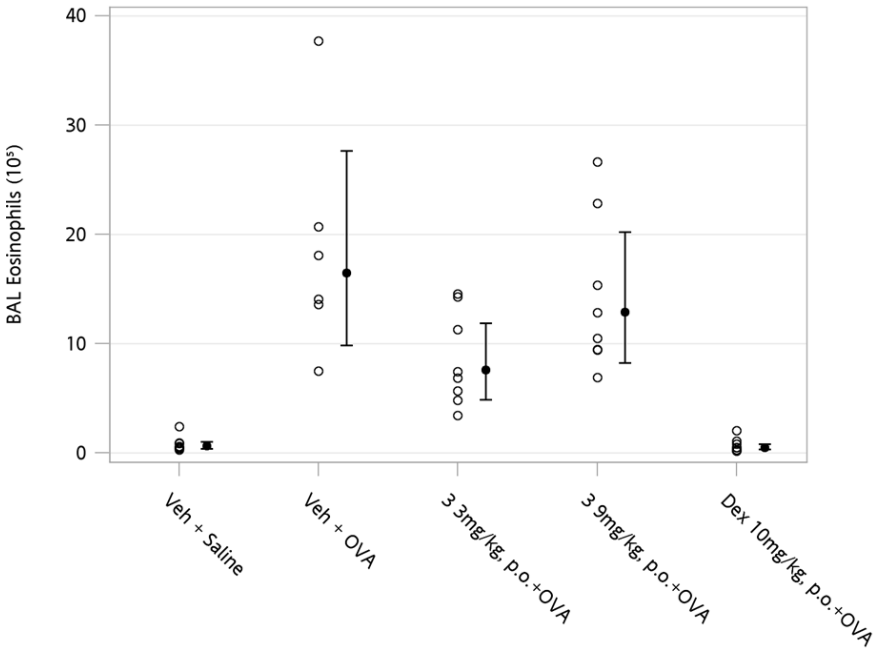

The data in Figure 6 was analysed using an analysis of variance model with the log eosinophil numbers as the response with treatment including the controls fitted as a categorical factor. The plotted intervals represent the 95% confidence interval of the mean response.

Table 6. Compiled pharmacokinetic data on compound **3** from pilot rat PK and PKPD studies

Dose (mg/kg)	Strain	AUC_{inf} (hr.ng/ml)	$T_{1/2}$ (hr)	Blood conc. 1hr (ng/ml (uM))	Unbound conc*. 1hr (uM)
1	WH	673	-	240 (0.52)	0.089
3	BN	454	10.6	86.9 (0.19)	0.032
9	BN	2621	6.8	586 (1.27)	0.22

*unbound concentration calculated using an internal algorithm that estimates binding from HPLC columns coated with HSA and α-glycoprotein.

Conclusions

Beginning with an inhaled start point with negligible oral bioavailability, a novel series of selective PI3Kδ inhibitors has been identified with a significantly improved pharmacokinetic profile. Key template modifications focused on controlling important physicochemical parameters revealed from analysis of data in the target biophase, with particular emphasis on number of aromatic rings, PSA and restricting hydrogen bond donors. Through a reduced complexity approach, the dihydroisobenzofuran chemotype was identified as a new hinge binding motif and subsequently elaborated through the creative application of [2+2+2] cyclo-trimerisation chemistry. This approach efficiently and rapidly led to identification of compound **3** which has good oral bioavailability, promising PI3K subtype selectivity, as well as highly encouraging levels of efficacy *in vivo*. Further evolution of this new series of PI3Kδ inhibitors will be reported in due course, with particular emphasis on enhancing the primary activity and selectivity profile, whilst maintaining acceptable pharmacokinetic properties.

Experimental

Chemistry. General. All solvents and reagents, unless otherwise stated, were commercially available from regular suppliers such as Sigma-Aldrich and Fluorochem and were used as purchased without further purification. Proton and carbon nuclear magnetic resonance (^{1}H NMR and ^{13}C NMR) spectra were recorded on a Bruker AVI (400 MHz), Bruker Nano (400 MHz), or Bruker AVII+ (600 MHz) spectrometer (with cryoprobe) in the indicated solvent. Chemical shifts δ are reported in parts per million (ppm) relative to tetramethylsilane and are internally referenced to the residual solvent peak. Coupling constants (*J*) are given in Hertz (Hz) to the nearest 0.1 Hz. High resolution mass spectra were obtained on a Micromass QTof Ultima hybrid quadrupole time-of-flight mass spectrometer, equipped with a Z-spray interface (ESI), over a mass range of 100 − 1100 Da, with a scan time of 0.9s and an interscan delay of 0.1 s. Reserpine was used as the external mass calibrant ([M + H]+ = 609.2812 Da). The Q-Tof Ultima mass spectrometer was operated in W reflectron mode to give a resolution (fwhm) of 16 000−20 000. Ionization was achieved with a spray voltage of 3.2 kV, a cone voltage of 50 V, with cone and desolvation gas flows of 10−20 and 600 L/h, respectively. The source block and desolvation temperatures were maintained at 120 and 250 °C, respectively. The elemental

composition was calculated using MassLynx, version 4.1, for the $[M + H]^+$ and the mass error quoted as ppm. LCMS methods are detailed in the Supporting Information. The purity of all compounds screened in the biological assays was examined by LCMS analysis and was found to be ≥95% unless otherwise specified.

N-(5-(1*H*-indazol-6-yl)-2-methoxypyridin-3-yl)methanesulfonamide (4)

N-(2-methoxy-5-(4,4,5,5-tetramethyl-1,3,2-dioxaborolan-2-yl)pyridin-3-yl)methanesulfonamide (218 mg, 0.66 mmol) and 6-bromo-1*H*-indazole (133 mg, 0.67 mmol) were introduced into a reaction tube and 2-Methyltetrahydrofuran (1.5 mL) added. Potassium fluoride (96.0 mg, 1.7 mmol) was dissolved in water (0.5 mL) and added into the mixture. The mixture was bubbled through with nitrogen for 4-5 mins then tri-*tert*-butylphosphonium tetra-fluoroborate (25 mg, 0.087 mmol) was mixed with Tris(dibenzylidene-acetone)dipalladium(0) (30 mg, 0.033 mmol) and added to the mixture. After 1 h, further Tri-tert-butyl-phosphonium tetra-fluoroborate (29 mg, 0.100 mmol) was mixed with Tris(dibenzylidene-acetone)dipalladium(0) (34 mg, 0.037 mmol) and added to the mixture.The resulting mixture was heated at reflux for 19 h before water (10 mL) and of 2-methyltetrahydrofuran (10 mL) was added. The organic phase was collected using a hydrophilic cartridge and then loaded onto a strong cation exchange (SCX, 20 g) cartridge. This was eluted with of MeOH (30 mL) and then of 2N NH_3/MeOH (90 mL). The NH_3/MeOH fraction was concentrated *in vacuo*. This sample was dissolved in DMSO (3 mL) and purified in 3 x 1 mL runs by mass directed autoprep on Xbridge column using acetonitrile/water with a formic acid modifier. The relevant fractions were combined and the solvent was removed under a stream of nitrogen to give **4** (59 mg, 28%).

LCMS (Method A): 0.74 min, $[M+H]^+$ 319 m/z. ^{1}H NMR (DMSO-d_6, 400 MHz) δ = 13.16 (s, 1H), 9.35 (br.s, 1H), 8.35 (d, *J* = 2.4, 1H), 8.08 (s, 1H), 7.94 (s, *J* = 2.4, 1H), 7.86 (s, *J* = 7.6, 1H), 7.71 (s, 1H), 7.39 (dd, *J* = 7.6, 1.5, 1H), 3.98 (s, 3H), 3.09 (s, 3H) ppm.

N-(5-(1,3-dihydroisobenzofuran-5-yl)-2-methoxypyridin-3-yl)methanesulfonamide (5)

N-(2-methoxy-5-(4,4,5,5-tetramethyl-1,3,2-dioxaborolan-2-yl)pyridin-3-yl)methanesulfonamide (0.074 g, 0.23 mmol), 5-bromo-1,3-dihydroisobenzofuran (0.030 g, 0.15 mmol), PdCl2(dppf)-CH_2Cl_2

adduct (2.5 mg, 3.00 μmol), cesium carbonate (0.072 g, 0.38 mmol) were combined in tetrahydrofuran (1 mL) and water (60 μL). The reaction vessel was sealed and heated in an Anton Parr microwave at 100 ºC for 25 min. The solution was then loaded onto C18 SPE (pre-conditioned with MeCN/0.1%TFA) and flushed through with a further 3 mLMeCN/0.1%TFA. Solvent was removed the residue dissolved in DMSO (0.5 mL) and purified by mass directed autoprep (MDAP) on Sunfire C18 column using acetonitrile/water with a formic acid modifier. The solvent was removed under a stream of nitrogen to give **5** (20.7 mg, 39%).

LCMS (Method A): 0.85 min, $[M+H]^+$ 321 m/z. ^{1}H NMR (DMSO-d_6, 400 MHz) δ = 9.35 (br.s, 1H), 8.26 (s, 1H), 7.83 (s, 1H), 7.57 (s, 1H), 7.53 (d, *J* = 7.6, 1H), 7.41 (d, *J* = 7.6, 1H), 5.09 (s, 2H), 5.05 (s, 2H), 3.95 (s, 3H), 3.06 (s, 3H) ppm.

N-(5-(3-hydroxy-3-methylbut-1-yn-1-yl)-2-methoxypyridin-3-yl)methanesulfonamide (19)

N-(5-bromo-2-methoxypyridin-3-yl)methanesulfonamide (7.03 g, 25 mmol) and copper(I) iodide (0.381 g, 2.00 mmol) were dissolved in anhydrous 2-methyltetrahydrofuran (80 mL) and nitrogen was bubbled into the mixture during 10 min at room temperature. Then, 2-methylbut-3-yn-2-ol (3.63 mL, 37.5 mmol), bis(triphenylphosphine)palladium(II) chloride (1.05 g, 1.50 mmol) and triethylamine (13.9 mL, 100 mmol) were added and the mixture stirred and heated. After 28 h at 85 ºC, the reaction exhibited approximately 60% conversion and 2-methylbut-3-yn-2-ol (1.2mL) and bis(triphenylphosphine)palladium(II) chloride (400 mg) added and stirred at 85 ºC for a further 17 h. Ammonium chloride (120 mL) and 2-methyltetrahydrofuran (80 mL) were added and the mixture filtered through celite. The layers were separated and the aqueous extracted with further 2-methyltetrahydrofuran (2 x 80 mL). The combined organics were washed with brine, dried over sodium sulfate and reduced *in vacuo*. The resulting residue was purified by column chromatography eluting with 0-100% ethyl acetate in cyclohexane. The approppriate fractions were combined and reduced in vacuo to provide **19** (7.39 g, 104%, contained residual ethyl acetate).

LCMS (Method A): 0.73 min, $[M+H]^+$ 285 m/z. ^{1}H NMR (acetone-d_6, 400 MHz) δ = 8.11 (br.s, 1H), 7.97 (d, *J* = 2.4, 1H), 7.73 (d, *J* = 2.4, 1H), 4.49 (s, 1H), 3.97 (s, 3H), 3.10 (s, 3H), 1.55 (s, 6H) ppm.

***N*-[5-ethynyl-2-(methyloxy)-3-pyridinyl]methanesulfonamide (13)**

Potassium hydroxide (9.87 g, 176 mmol) was dissolved in isopropanol (80 mL) at 50ºC over 10 minutes then **19** (10 g, 35.2 mmol) added in isopropanol (80 mL + 40 mL wash). The mixture was heated to reflux (90 ºC) for 4 1/2 hours. Another 0.5 equivalent of potassium hydroxide (0.968 g) was added, and the reaction was stirred under reflux (95 ºC) for a further 4 h. The reaction was allowed to stand at room temperature for 18 h then reduced *in vacuo* and partitioned between aqueous ammonium chloride (150 mL) and 2-methyl tetrahydrofuran (100 mL). The aqueous layer was washed with 2-methyl tetrahydrofuran (2 x 100 mL) and the combined organics washed with brine, dried over sodium sulfate and reduced *in vacuo*. The resulting residue was purified by column chromatography eluting with 0-50% ethyl acetate in cyclohexane to give **13** (5.0 g, 60%).

LCMS (Method A): 0.74 min, $[M+H]^+$ 227 m/z. ^{1}H NMR (acetone-d_6, 400 MHz) δ = 8.5 (br.s, 1H), 8.08 (d, *J* = 2.4, 1H), 7.82 (d, *J* = 2.4, 1H), 4.01 (s, 3H), 3.74 (s, 1H), 3.12 (s, 3H) ppm.

***N*-{2-(Methyloxy)-5-[7-(trimethylsilyl)-1,3-dihydro-2-benzofuran-5-yl]-3-pyridinyl}methanesulfonamide (14)**

Proceedure A. To a nitrogen degassed solution of chloro(pentamethylcyclopentadienyl)(cyclooctadiene)ruthenium(II) (38 mg, 0.1 mmol) and N-[5-ethynyl-2-(methyloxy)-3-pyridinyl]methanesulfonamide (226 mg, 1.0 mmol) in CPME (7.5 mL) was added a solution of **13** (200 mg, 1.20 mmol) in CPME (7.5 mL) sequentially, dropwise at room temperature. The mixture was then stirred at room temperature for 24 h. The mixture was concentrated under reduced pressure to afford a crude gum. The gum was loaded in minimal CH_2Cl_2 onto a silica pre-packed column (10 g) and eluted with 0-100% EtOAc in cyclohexane over 60 min. The combined relevant fractions were concentrated under reduced pressure to give **14** (250 mg, 64%) as a white solid.

Proceedure B. To chloro(pentamethylcyclopentadienyl)(cyclooctadiene)ruthenium(II) (344 mg, 902 µmol) was added a solution of **13** (4.1 g, 18 mmol) in CPME (65 mL) and the mixture was degassed with three alternative applications of vacuum and nitrogen. To the mixture was added a solution of

trimethyl[3-(2-propyn-1-yloxy)-1-propyn-1-yl]silane (1.5 g, 9.0 mmol) in CPME (40 mL) sequentially, dropwise at room temperature. The reaction mixture was then stirred at room temperature for 2 h. The reaction mixture was diluted with ethyl acetate (100 mL) and washed with brine (3 x 50 mL). The aqueous extracts were back extracted with ethyl acetate (50 mL). The combined organic extracts were dried under reduced pressure to afford a crude gum. The gum was loaded in minimal CH_2Cl_2 onto a silica pre-packed column (340 g) and eluted with 0-10% EtOAc in CH_2Cl_2 over 12 column volumes. The combined relevant fractions were concentrated under reduced pressure to give **14** (2.26 g, 5.76 mmol, 64 % yield) as a yellow solid.

m.p. 166 - 167 °C. LCMS (Method A): 1.19 min, $[M+H]^+$ 393 m/z. IR (solid) 3171 (N-H stretch); 1327, 1137 (O=S=O) cm^{-1}. ^1H NMR (DMSO-d_6, 400 MHz) δ = 9.33 (s, 1H), 8.28 (d, *J* = 2.3 Hz, 1H), 7.85 (d, *J* = 2.3 Hz, 1H), 7.57 (s, 1H), 7.54 (s, 1H), 5.09 (s, 2H), 5.05 (s, 2H), 3.97 (s, 3H), 3.08 (s, 3H), 0.30 (s, 9H) ppm. ^{13}C NMR (DMSO-d_6, 101 MHz): δ = 157.2, 144.5, 141.5, 140.3, 136.4, 134.2, 132.2, 132.1, 131.2, 122.4, 121.3, 73.9, 73.3, 54.8, 41.8, 0.0 ppm. HRMS (ESI) calc'd for $C_{18}H_{25}N_2O_4SSi$ $[M+H]^+$ 393.1299, found 393.1298.

***N*-[5-(7-Iodo-1,3-dihydro-2-benzofuran-5-yl)-2-(methyloxy)-3-pyridinyl]methanesulfonamide (15)**

Iodine monochloride in CH_2Cl_2 (1 M, 4.33 mL, 4.33 mmol) was added dropwise to a solution of **14** (850 mg, 2.17 mmol) in CH_2Cl_2 (20 mL) under nitrogen at -10 ºC. The reaction mixture was allowed to warm to 0 ºC and stirred for 5 minutes, during which a white solid precipitated from solution. Saturated sodium thiosulfate solution (50 mL) was added and the resulting mixture stirred at room temperature for 20 min. The reaction mixture was filtered under reduced pressure and washed with CH_2Cl_2 (5 mL). The filtrate was poured onto CH_2Cl_2 (50 mL) and water (30 mL) and the separated aqueous phase was extracted with CH_2Cl_2 (2 x 50 mL). The combined organic fractions were passed through a hydrophobic frit then concentrated under vacuum to afford a yellow solid. The yellow solid and white solid were combined and triturated in methanol (5 mL). The mixture was filtered under reduced pressure and the solid was dried in a vacuum oven for 2 h to afford **15** (774 mg, 1.73 mmol,

80%) as a white solid. LCMS (Method A): 1.06 min, $[M+H]^+$ 447 m/z. ^{1}H NMR (DMSO-d_6, 400 MHz): δ = 9.26 - 9.39 (m, 1H), 8.28 (d, *J* = 2.3 Hz, 1H), 7.89 (s, 1H), 7.85 (d, *J* = 2.3 Hz, 1H), 7.59 (s, 1H), 5.21 (s, 2H), 4.92 (s, 2H), 3.96 (s, 3H), 3.09 (s, 3H) ppm. ^{13}C NMR (101 MHz, DMSO-d_6): δ = 156.8, 143.2, 141.5, 141.1, 138.8, 134.3, 131.0, 128.8, 121.9, 119.8, 89.0, 76.9, 74.7, 54.3, 41.2 ppm.

***N*-(5-(7-Amino-1,3-dihydroisobenzofuran-5-yl)-2-methoxypyridin-3-yl)methanesulfonamide (16)**

L-proline (413 mg, 3.59 mmol), copper(I) iodide (68 mg, 0.36 mmol), cesium carbonate (1.75 g, 5.38 mmol) and **15** (800 mg, 1.79 mmol) were evenly charged over 2 microwave vials (2 x 20 mL). The vials was sealed and degassed before aqueous ammonia solution 0.88 (35%, 8.0 mL, 0.13 mol) and DMSO (8 mL) were added *via* syringe and the vials were heated and stirred in a Biotage microwave reactor at 50 ºC for 2 h. After this time aqueous ammonia solution 0.88 (35%, 2 x 4 mL, 0.2 mol) and cesium carbonate (2 x 500 mg, 1.53 mmol) was added *via* syringe to both vials and the vials were heated and stirred at 110 ºC for 6 h. The reaction mixtures were combined and filtered under reduced pressure, then washed with methanol. The filtrate was loaded directly onto a SCX cartridge (70 g) and flushed with methanol (200 mL) under reduced pressure. The column was then eluted with ammonia in methanol solution (7 M, 300 mL) under reduced pressure. The filtrate was concentrated under reduced pressure to afford a crude gum. The gum was dissolved in CH_2Cl_2 (30 mL) and washed three times with water. The combined organic fractions were filtered through a hydrophobic frit and concentrated under reduced pressure to afford **16** (460 mg, 1.37 mmol, 77%) as a white solid. m.p. 295 - 301 °C. LCMS (Method A): 0.65 min, $[M+H]^+$ 336 m/z. IR (solid) 3467, 3377 (H-N-H stretch); 3049 (N-H stretch); 1303, 1138 (O=S=O) cm^{-1}. ^{1}H NMR (DMSO-d_6, 400 MHz): δ = 9.28 (br. s., 1H), 8.17 (d, *J* = 2.3 Hz, 1H), 7.77 (d, *J* = 2.3 Hz, 1H), 6.64 - 6.78 (m, 2H), 5.25 (s, 2H), 4.97 (s, 2H), 4.88 (s, 2H), 3.96 (s, 3H), 3.07 (s, 3H) ppm. ^{13}C NMR (DMSO-d_6, 101 MHz): δ = 155.8, 142.9, 140.8, 140.0, 137.1, 130.6, 130.5, 122.3, 121.1, 110.7, 106.6, 73.2, 71.5, 53.7, 40.6 ppm. HRMS (ESI) calc'd for $C_{15}H_{18}N_3O_4S$ $[M+H]^+$ 336.1013, found 336.1017.

_N_-(2-Methoxy-5-(7-(5-methyl-1,3,4-oxadiazol-2-yl)-1,3-dihydroisobenzofuran-5-yl)pyridin-3-yl)methanesulfonamide (6)

A microwave vial was charged with 2-methyl-1,3,4-oxadiazole (45 mg, 0.54 mmol) and THF (1.5 mL). Zinc chloride (244 mg, 1.79 mmol) was added and the mixture was degassed and cooled to -10 ºC under nitrogen. A solution of lithiumhexamethyldisilazide in THF (1 M, 810 µL, 810 µmol) was then added dropwise over 15 min at -10 °C. The resulting mixture was stirred at -10 °C (+/-5 °C) for 1 h. **15** (200 mg, 450 µmol), tetrakis(triphenylphosphine)palladium(0) (52 mg, 45 µmol) and cesium carbonate (146 mg, 448 µmol) were then added at -10 °C. The mixture was then degassed with three alternative applications of vacuum and nitrogen, then heated in a Biotage microwave at 150 ºC for 1 h. The mixture was poured onto CH_2Cl_2 (20 mL) and the mixture was filtered under reduced pressure. The filtrate was extracted with CH_2Cl_2 (3 x 50 mL) and the combined organic phase was treated with water (50 mL). The resulting mixture was filtered under reduced pressure and washed with CH_2Cl_2 (3 x 50 mL). The filtrate was passed through a hydrophobic frit and then concentrated under reduced pressure to afford a yellow solid. The solid was loaded in DMSO (1 mL) and purified *via* mass directed auto-preparative (MDAP) chromatography using a Sunfire C18 column and an ammonium bicarbonate-modified MeCN/water gradient. The relevant combined fractions were concentrated under reduced pressure to give **6** (45 mg, 0.11 mmol, 24%) as a white solid. LCMS (Method A): 0.78 min, $[M+H]^+$ 403. IR (solid) 2929 (N-H stretch); 1331, 1149 (O=S=O) cm^{-1}. ^1H NMR (DMSO-d_6, 400 MHz): δ = 9.37 (s, 1H), 8.37 (d, *J* = 2.3 Hz, 1 H), 8.02 (d, *J* = 1.3 Hz, 1H), 7.94 (d, *J* = 2.3 Hz, 1H), 7.84 (s, 1H), 5.34 (s, 2H), 5.17 (s, 2H), 3.99 (s, 3H), 3.10 (s, 3H), 2.62 (s, 3H) ppm. ^{13}C NMR (101 MHz, DMSO-d_6) δ = 164.4, 163.3, 156.9, 142.7, 140.6, 137.8, 137.7, 130.6, 129.1, 123.7, 122.8, 122.6, 118.5, 73.9, 73.0, 54.3, 41.2, 11.1 ppm. HRMS (ESI) calc'd for $C_{18}H_{19}N_4O_5S$ $[M+H]^+$ 403.1071, found 403.1070.

_N_-(2-Methoxy-5-(7-(pyridin-2-yl)-1,3-dihydroisobenzofuran-5-yl)pyridin-3-yl)methanesulfonamide (7)

A microwave vial was charged with **15** (70 mg, 0.16 mmol), 2-(4,4,5,5-tetramethyl-1,3,2-dioxaborolan-2-yl)pyridine (80 mg, 0.39 mmol), cesium carbonate (102 mg, 0.310 mmol), copper(I) chloride (16 mg, 0.16 mmol), palladium(II) acetate (0.5 mg, 2 μmol), 1,1'-bis(diphenylphosphino)ferrocene (dppf) (18 mg, 30 μmol) and DMF (1.5 mL). The vial was sealed and degassed then heated and stirred in a Biotage microwave reactor at 100 ºC for 90 min. The mixture was poured onto water (20 mL) and EtOAc (20 mL) and the mixture was then filtered under reduced pressure. The separated aqueous phase was extracted with EtOAc (3 x 20 mL) and the combined organic phase was filtered. The filtrate was concentrated under reduced pressure to afford a brown solid. The solid was loaded in DMSO/MeOH solution (1:1 (v/v) 1 mL) and purified *via* mass directed auto-preparative (MDAP) chromatography using a Sunfire C18 column and an ammonium bicarbonate-modified MeCN/water gradient. The relevant combined fractions were concentrated under reduced pressure to give **7** (6 mg, 0.02 mmol, 10%) as a white solid. LCMS (Method A): 0.89 min, $[M+H]^+$ 398 m/z. ^{1}H NMR (DMSO-d_6, 400 MHz,) δ = 9.07-9.43 (m, 1H), 8.70 (d, *J* = 4.03 Hz, 1H), 8.41 (d, *J* = 2.01 Hz, 1H), 8.06 (s, 2H), 7.90-8.00 (m, 2H), 7.65 (s, 1H), 7.39 (dd, *J* = 5.16, 6.92 Hz, 1H), 5.38 (s, 2H), 5.11 (s, 2H), 3.99 (s, 3H), 3.09 (s, 3H) ppm.

_N_-(6-(6-Methoxy-5-(methylsulfonamido)pyridin-3-yl)-1,3-dihydroisobenzofuran-4-yl)acetamide (8)

Acetic acid (10 μL, 0.15 mmol) was added dropwise to a stirred suspension of HATU (62 mg, 0.16 mmol) and DIPEA (50 μL, 0.30 mmol) in CH_2Cl_2 (1 mL) at room temperature. The mixture was stirred for 10 min at room temperature, during which time the milky suspension turned into a yellow solution. A suspension of **16** (50 mg, 0.15 mmol) in CH_2Cl_2 (1 mL) was then added dropwise to the mixture at room temperature. DMF (10 μL) was added and the solution was stirred for 16 h at room temperature. The solution was poured onto EtOAc (2 mL) and brine (3 mL) and the separated organic phase was washed with brine (2 x 3 mL). The combined organic phase was concentrated under a stream of nitrogen to give an orange gum. The gum was dissolved in DMSO/MeOH (1 mL, 1:1 v/v) and purified *via* mass directed auto-preparative (MDAP) chromatography using a Sunfire C18 column and an ammonium bicarbonate-modified MeCN/water gradient. The relevant combined fractions

were concentrated under reduced pressure to give a white solid. Water (10 mL) and diethyl ether (10 mL) was added and the mixture filtered and the filter cake was dried under reduced pressure to give **8** (12 mg, 30 μmol, 21%) as a white solid. m.p. 225 - 228 °C. LCMS (Method A): 0.67 min, $[M+H]^+$ 378 m/z. IR (solid) 3240 (N-H stretch); 3080 (N-H stretch); 1629 (C=O); 1321, 1144 (O=S=O) cm^{-1}.^{1}H NMR (DMSO-d_6, 400 MHz): δ = 9.77 (s, 1H), 9.37 (s, 1H), 8.23 (s, 1H), 7.81 (s, 1H), 7.65 (s, 1H), 7.34 (s, 1H), 5.05 (s, 2H), 4.96 (s, 2H), 3.96 (s, 3H), 3.07 (s, 3H), 2.07 (s, 3H) ppm. ^{13}C NMR (101 MHz, DMSO-d_6) δ = 168.3, 156.1, 141.6, 140.3, 136.6, 132.9, 130.7, 130.4, 129.6, 121.3, 118.9, 115.0, 72.8, 72.1, 53.8, 40.7, 23.4 ppm. HRMS (ESI) calc'd for $C_{17}H_{20}N_3O_5S$ $[M+H]^+$ 378.1118, found 378.1120.

***N*-(6-(6-Methoxy-5-(methylsulfonamido)pyridin-3-yl)-1,3-dihydroisobenzofuran-4-yl)-2-methylthiazole-4-carboxamide (9)**

DIPEA (50 μL, 0.30 mmol) and HATU (62 mg, 0.16 mmol) were added sequentially to a stirred solution of 2-methyl-1,3-thiazole-4-carboxylic acid (34 mg, 24 μmol) in DMF (0.5 mL) at room temperature and the solution stirred for 10 min. A solution of **16** (50 mg, 0.15 mmol) in DMF (0.5 mL) was then added dropwise at room temperature and the solution stirred at room temperature for 16 h, during which time a white solid precipitated. The mixture was filtered under reduced pressure and washed with water (10 mL) then diethyl ether (10 mL). The white solid was dried in a vacuum oven for 16 h to afford **9** (23.5 mg, 50.0 μmol, 21%) as a white solid. m.p. 274 - 277 °C. LCMS (Method A): 0.89 min, $[M+H]^+$ 461 m/z. IR (solid) 3379 (N-H stretch); 3141 (N-H stretch); 1671 (C=O); 1324, 1136 (O=S=O) cm^{-1}. ^{1}H NMR (DMSO-d_6, 400 MHz): δ = 10.30 (s, 1H), 9.39 (s, 1H), 8.25 - 8.44 (m, 2H), 7.93 (d, *J* = 2.3 Hz, 1H), 7.71 (s, 1H), 7.49 (s, 1H), 5.15 (s, 2H), 5.07 (s, 2H), 4.03 (s, 3H), 3.14 (s, 3H), 2.83 (s, 3H) ppm. ^{13}C NMR (DMSO-d_6, 101 MHz): δ = 166.2, 158.8, 156.0, 148.7, 142.1, 140.1, 136.9, 132.6, 132.1, 130.6, 129.3, 125.4, 121.5, 120.8, 115.8, 72.7, 72.2, 53.7, 40.7, 18.8 ppm. HRMS (ESI) calc'd for $C_{20}H_{21}N_4O_5S_2$ $[M+H]^+$ 461.0948, found 461.0951.

***N*-(6-(6-Methoxy-5-(methylsulfonamido)pyridin-3-yl)-1,3-dihydroisobenzofuran-4-yl)-2-morpholinoacetamide (3)**

DIPEA (80 µL, 0.48 mmol) and HATU (100 mg, 260 µmol) were added sequentially to a stirred solution of morpholin-4-yl-acetic acid (35 mg, 0.24 mmol) in DMF (0.5 mL) at room temperature. The reaction was stirred for 10 min at room temperature. A solution of **16** (80 mg, 0.24 mmol) in DMF (0.5 mL) was then added dropwise to the reaction mixture at room temperature and the mixture was stirred at room temperature for 16 h. The mixture was poured onto EtOAc (2 mL) and brine (3 mL) and the separated organic phase was washed with brine (2 x 3 mL). The combined organic phase was concentrated under a stream of nitrogen to give an orange gum. The gum was dissolved in DMSO/MeOH (1 mL, 1:1 v/v) and purified *via* mass directed auto-preparative (MDAP) chromatography using a Sunfire C18 column and an ammonium bicarbonate-modified MeCN/water gradient. The relevant fractions were combined and the volume reduced by 70% under a stream of nitrogen. A white solid precipitated from solution. The mixture was filtered under reduced pressure and washed with water (10 mL) then diethyl ether (10 mL) and then dried in a vacuum oven for 1 hour to afford **3** (25 mg, 50 µmol, 22%) as a white solid. m.p. 218 - 220 °C. LCMS (Method A): 0.54 min, $[M+H]^+$ 463 m/z. IR (solid) 3224 (N-H stretch); 2925 (N-H stretch); 2852 (C-H stretch); 1658 (C=O); 1318, 1142 (O=S=O) cm^{-1}. ^1H NMR (DMSO-d_6, 400 MHz): δ = 9.63 (s, 1H), 9.24 - 9.46 (m, 1H), 8.24 (d, *J* = 2.3 Hz, 1H), 7.83 (d, *J* = 2.3 Hz, 1H), 7.67 (s, 1H), 7.37 (s, 1H), 5.07 (s, 2H), 4.98 (s, 2H), 3.96 (s, 3H), 3.65 (t, *J* = 4.5 Hz, 4H), 3.15 (s, 2H), 3.07 (s, 3H), 2.53 (t, *J* = 4.5 Hz, 4H) ppm. ^{13}C NMR (DMSO-d_6, 101 MHz): δ = 168.0, 156.1, 141.6, 140.3, 136.6, 133.1, 130.7, 130.4, 129.6, 121.3, 118.8, 115.0, 72.8, 72.1, 53.8, 40.7, 40.2, 38.9, 23.4 ppm. HRMS (ESI) calc'd for $C_{21}H_{27}N_4O_6S$ $[M+H]^+$ 463.1651, found 463.1656.

***N*-(6-(6-Methoxy-5-(methylsulfonamido)pyridin-3-yl)-1,3-dihydroisobenzofuran-4-yl)-6-methylpicolinamide (10)**

DIPEA (50 µL, 0.30 mmol) and HATU (62 mg, 0.16 mmol) were added sequentially to a stirred solution of 6-methylpicolinic acid (33 mg, 0.24 mmol) in DMF (0.5 mL) at room temperature and the solution stirred for 10 min. A solution of **16** (50 mg, 0.15 mmol) in DMF (0.5 mL) was then added dropwise at room temperature and the mixture stirred at room temperature overnight. The reaction mixture was poured onto EtOAc (2 mL) and brine (3 mL) and the separated organic phase was

washed with brine (2 x 3 mL). The combined organic phase was concentrated under a stream of nitrogen to give an orange gum. The gum was loaded in a solution of DMSO/MeOH (1 mL, 1:1 v/v) and purified *via* mass directed auto-preparative (MDAP) chromatography using a Sunfire C18 column and an ammonium bicarbonate-modified MeCN/water gradient. The relevant fractions were combined and concentrated under a stream of nitrogen to give **10** (30 mg, 60 μmol, 28%) as a white solid. LCMS (Method A): 0.99 min, $[M+H]^+$ 455 m/z. ^{1}H NMR (DMSO-d_6, 400 MHz): δ = 10.49 (s, 1H), 9.26 - 9.57 (br. s, 1H), 8.31 (d, *J* = 2.3 Hz, 1H), 7.94 - 7.99 (m, 2H), 7.89 (d, *J* =2.3 Hz, 1H), 7.81 (s, 1H), 7.56 (dd, *J* = 6.2, 2.4 Hz, 1H), 7.46 (s, 1H), 5.11 (s, 2H), 5.07 (s, 2H), 3.98 (s, 3H), 3.09 (s, 3H), 2.64 (s, 3H) ppm.

Biology. PI3Kα, -β, -γ, and -δ HTRF Assays. Inhibition of PI3 Kinase enzymatic activity was determined using a homogeneous time-resolved fluorescence (HTRF) kit assay format provided by Millipore. Reactions were performed in assay buffer containing 50 mM HEPES, pH 7.0, 150 mM NaCl, 10 mM $MgCl_2$, <1% cholate (w/v), <1% CHAPS (w/v), 0.05% sodium azide (w/v), and 1 mM DTT. Enzymes were preincubated with compound, serially diluted 4-fold in 100% DMSO, for 15 min prior to reaction initiation upon addition of substrate solution containing ATP at K_m for the specific isoform tested (α at 250 μM, β at 400 μM, δ at 80 μM, and γ at 15 μM), PIP2 at either 5 μM (PI3Kδ) or 8 μM (PI3Kα, -β, and -γ) and 10 nM biotin-PIP3. Assays were quenched after 60 min by addition of a quench/detection solution prepared in 50 mM HEPES, pH 7.0, 150 mM NaCl, <1% cholate, <1% Tween 20, 30 mM EDTA, 40 mM potassium fluoride, and 1 mM DTT containing 16.5 nM GRP- 1 PH domain, 8.3 nM streptavidin-APC, and 2 nM europium-antiGST and were left for a further 60 min in the dark to equilibrate prior to reading using a BMG RubyStar plate reader. Ratio data were normalized to high (no compound) and low (no enzyme) controls prior to fitting using a logistical four-parameter equation to determine IC_{50}.

Peripheral Blood Mononuclear (PBMC) Assay. Reagents were purchased from Invitrogen Corporation Ltd. unless otherwise specified. PBMC cells (peripheral blood mononuclear cells) were prepared from heparinized human blood (using 1% v/v heparin sodium 1000 U/mL endotoxin free, Leo Laboratories Ltd.) using the Accuspin system-Histopaque-1077 (Sigma-Aldrich Company Ltd.).

The cells were resuspended in RPMI1640 medium containing 10% fetal calf serum, 1% L-glutamine, and 1% penicillin/streptomycin. The cells at a density of 5 × 105 viable cells/mL were incubated with 0.0156% (v/v) CytoStim (Miltenyi Biotech). The assay plate was then incubated at 37 °C, 5% CO_2, for 20 h. The supernatant was removed, and the concentrations of IFNγ were determined by electrochemiluminescence assay using the Meso Scale Discovery (MSD) technology (Meso Scale Discovery).

Brown Norway Rat Acute OVA Model of Th2 Driven Lung Inflammation. All reagents unless stated were from Sigma-Aldrich. The models used in these studies conform to U.K. standards of animal care, as laid down by the Home Office. Procedures were carried out as exactly specified under GlaxoSmithKline's Respiratory Diseases Project license (PPL 80/2361 and 80/1537). Male brown Norway (BN) rats, weighing 250−300 g were sensitized by intraperitoneal injection of a 1 mL OVA solution containing 10 μg of OVA and 20 mg of $Al(OH)_3$ on days 1 and 7. On day 21 or 28, rats were challenged with 0.2 mL of intratracheal OVA solution under isoflurane (Abbott Laboratories) anesthesia. Compound in vehicle (0.2% Tween 80, water, pH 4.5) or vehicle alone was also dosed by i.t. route (0.2 mL volume) at t − 30 min and +24 h relative to intratracheal OVA challenge. 48 h after i.t. OVA challenge rats were sacrificed by anesthetic overdose. The trachea was exposed and lungs were lavaged with 5 mL of lavage fluid (0.1% BSA, 10 mM EDTA, and 1 protease inhibitor tablet, catalog no. 11873580001 from Roche, per 50 mL). Death was confirmed by cervical dislocation. BAL was immediately transferred onto ice, and leucocytes were then quantified by flow cytometry. Briefly, samples were read on a BD FACSCANTO II 8 color flow cytometer. Lymphocytes, eosinophils, neutrophils, and macrophages were gated on FSC and SSC using morphological criteria. Threshold was set on FSC channel. In some studies the Amcyan channel was used to gate cells further using autofluorescence (intersecting gates). DAPI+ cells were excluded as dead. For cytokine analysis mice were lavaged 24 h after OVA challenge. BAL was spun at 4 °C at 300g for 7 min and the supernatant stored at 20 °C prior to analysis. Data from repeat studies were average-standardized, pooled, and a four-parameter nonlinear logistic curve was fitted.

Pharmacokinetic Studies. *In vitro* clearance was determined to assess metabolic stability of compounds in rat microsomes. Microsomes (190 μL, 0.5 mg of protein/mL) were prewarmed for 10 min at 37 °C. The incubation was initiated by addition of NADPH regeneration system (50 μL) and compound (10 μL, 12.5 μM), resulting in a final compound concentration of 0.5 μM in the incubation. Samples (20 μL) were removed at 0, 3, 6, 12, and 30 min, and the reaction was quenched by addition to acetonitrile (100 μL) containing internal standard (IS). Compound remaining was measured using specific LC−MS/MS methods as a ratio to the internal standard in the absence of a calibration curve. Peak area ratios (compound to IS) were fitted to an unweighted logarithmic decline in substrate. By use of the first order rate constant, clearance was calculated by adjustment for protein concentration (0.5 mg/mL), volume of the incubation (250 μL), and hepatic scaling factor (52.5 mg of microsomal protein/g of liver). HSA binding was measured *via* chormatographic analysis according to the published methodology.[32] Passive membrane permeability was determined in MDCKII-MDR1 cells, at pH 7.4 in the presence of a potent P-glycoprotein inhibitor. Each compounds was incubated in duplicate at a concentration of 3 *m*M on one test occasion. In this assay the passive apparent permeability (P_{app}) is reported in nm/sec (single test occasion). *In vivo* pharmacokinetics was tested in Sprague Dawley male rats. Compounds were administered discretely by the oral and intravenous routes at dose levels of 3 and 1 mg/kg, respectively (n = 2 rats/route). Compounds were formulated as a solution in DMSO/PEG200/water (5:45:50 v/v/v) at a dose volume of 6 (oral) and 2 (intravenous) mL/ kg. All animals were serially bled from the tail vein, and blood samples collected over a time-course of 0−7 h were submitted to LC−MS/MS analysis for the quantification of the parent compound. The main pharmacokinetic parameters were estimated by noncompartmental analysis.

Chemiluminescent Nitrogen Detection (CLND) Solubility Determination. GSK in-house kinetic solubility assay involved the following: 5 mL of 10 mM DMSO stock solution diluted to 100 μL with pH 7.4 phosphate buffered saline, equilibrated for 1 h at room temperature, filtered through Millipore Multiscreen HTS-PCF filter plates (MSSL BPC). The filtrate was quantified by suitably calibrated flow injection chemiluminescent nitrogen detection.[33] The standard error of the CLND solubility

determination was ±30 μM, and the upper limit of the solubility is 500 μM when working from 10 mM DMSO stock solution.

All animal studies were ethically reviewed and carried out in accordance with Animals (Scientific Procedures) Act 1986 and the GSK Policy on the Care, Welfare and Treatment of Laboratory Animals. The human biological samples were sourced ethically, and their research use was in accord with the terms of the informed consents.

Footnotes:

*Corresponding author e-mail: simon.2.peace@gsk.com, telephone: (+44)1438551573

[a]D. Perez present address: 2M Aurochs INDUSTRIE, ZI de la Plaine, 3 Impasse du Lac, 31140 Aucamville, Fr.

All authors were employees of GlaxoSmithkline or University of Strathclyde at the time the research was carried out.

The corresponding author wishes to dedicate this manuscript to Dr Robert Ife.

Compound **3** PDB accssion code 5L72. The authors will release the atomic coordinates and experimental data upon article publication.

References

(1) Ghigo, A.; Damilano, F.; Braccini, L.; Hirsch, E. PI3K inhibition in inflammation: Toward tailored therapies for specific diseases. *BioEssays* **2010**, 32, *3*, 185-196.

(2) Chen, K.; Iribarren, P.; Gong, W.; Wang, J. M. The essential role of phosphoinositide 3-kinases (PI3Ks) in regulating pro-inflammatory responses and the progression of cancer. *Cell. & Mol. Immun*. **2005**, *2*, 241-252.

(3) Paz-Ares, L.; Blanco-Aparicio, C.; Garcia-Carbonero, R.; Carnero, A. Inhibiting PI3K as a therapeutic strategy against cancer. *Clin. Transl. Oncol.* **2009**, *11*, 9, 572-579.

(4) Czech, M. P. PIP2 and PIP3: complex roles at the cell surface. *Cell* **2000**, *100*, 603–606.

(5) Soond, D. R.; Bjørgo, E.; Moltu, K.; Dale, V. Q.; Patton, D. T.; Torgersen, K. M.; Galleway, F.; Twomey, B.; Clark, J.; Gaston, JS. H.; Taskén, K.; Bunyard, P.; Okkenhaug, K. PI3K p110δ regulates T cell cytokine production during primary and secondary immune responses in mice and humans. *Blood*, **2010**, *115*, 2203-2213.

(6) Brown, J. M.; Wilson, T. M.; Metcalfe, D. D. The mast cell and allergic diseases: role in pathogenesis and implications for therapy. *Clin. Exp. Allergy*, **2007**, *38*, 4-18.

(7) Sadhu, C.; Masinovsky, B.; Dick, K.; Sowell, C. G.; Staunton, D. E. Essential role of phosphoinositide 3-kinase δ in neutrophil directional movement. *J. Immunol*. **2003**, *170*, 2647-2654.

(8) Condliffe, A.M.; Davidson, K.; Anderson, K.E.; Ellson C.D.; Crabbe, T.; Okkenhaug, K.; Vanhaesebroeck, B.; Turner, M.; Webb, L.; Wymann, M.P.; Hirsch, E.; Ruckle, T.; Camps, M.; Rommel, C.; Jackson, S.P.; Chilvers, E.R.; Stephens, L.R.; Hawkins, P.T. Sequential activation of class IB and class IA PI3K is important for the primed respiratory burst of human but not murine neutrophils *Blood*. **2005,** *106*, 1432-1440.

(9) Rowan, W. C.; Smith, J. L.; Affleck, K.; Amour, A. Targeting phosphoinositide 3-kinase δ for allergic asthma. *Biochem. Soc. Trans.* **2012**, *40*, 240-245.

(10) Sriskantharajah, S.; Hamblin, N.; Worsley, S.; Calver, A. R.; Hessel, E. M.; Amour , A. Targeting phosphoinositide 3-kinase δ for the treatment of respiratory diseases. *Ann. N. Y. Acad. Sci.* **2013**, *1280*, 35-39.

(11) Ball, J.; Archer, S.; Ward, S. PI3K inhibitors as potential therapeutics for autoimmune disease. *Drug Discov. Today* **2014**, *19*, 1195-1199.

(12) Vanhaesebroeck, B.; Ali, K.; Bilancio, A.; Geering, B.; Foukas, L. C. Signalling by PI3K isoforms: insights from gene-targeted mice. *Trends Biochem. Sci.* **2005**, *30*, 194-204.

(13) Rückle, T.; Schwarz, M. K.; Rommel, C. PI3Kγ inhibition: towards an 'aspirin of the 21st century'? *Nat. Rev. Drug Discov.* **2006**, *5*, 903-18.

(14) Down, K., Amour, A., Baldwin, I. R.; Cooper, A. J. W., Deakin, A. M., Felton, L.M., Guntrip, S. B.; Hardy, C., Harrison, Z. A.; Jones, K.L., Jones, P.; Keeling, S. E.; Le, J.; Livia, S.; Lucas, F.;

Lunniss, C. J.; Parr, N. J.; Robinson, E.; Rowland, P.; Smith, S.; Thomas, D. A.; Vitulli, G.; Washio, Y.; Hamblin, J. N. Optimization of Novel Indazoles as Highly Potent and Selective Inhibitors of Phosphoinositide 3-Kinase δ for the Treatment of Respiratory Disease. *J. Med. Chem*. **2015**, *58*, 7381−7399.

(15) Winkler, D. G.; Faia, K. L; DiNitto, J. P.; Ali, J. A.; White, K. F.; Brophy, E. E.; Pink, M. M.; Proctor, J. L.; Lussier, J.; Martin, C. M.; Hoyt, J. G.; Tillotson, B.; Murphy, E. L.; Lim, A. R.; Thomas, B. D.; MacDougall, J. R.; Ren, P.; Liu, Y.; Li, L. S.; Jessen, K. A.; Fritz, C. C.; Dunbar, J. L.; Porter, J. R.; Rommel, C.; Palombella, V. J.; Changelian, P. S.; Kutok , J. L. PI3K-δ and PI3K-γ inhibition by IPI-145 abrogates immune responses and suppresses activity in autoimmune and inflammatory disease models. *Chem. Biol.* **2013**, *20*, 1364-1374.

(16) (i) Lannutti, B. J.; Meadows, S.A.; Herman, S. E, Kashishian, A., Steiner, B.; Johnson, A. J.; Byrd, J. C.; Tyner, J. W.; Loriaux, M. M.; Deininger, M.; Druker, B. J.; Puri, K. D.; Ulrich, R. G.; Giese, N. A. CAL-101, a p110delta selective phosphatidylinositol-3-kinase inhibitor for the treatment of B-cell malignancies, inhibits PI3K signaling and cellular viability.

Blood. **2011**, *117*, 591-594. (ii) Furman, R. R.; Sharman, J. P.; Coutre, S. E.; Cheson, B. D.; Pagel, J. M.; Hillmen, P.; Barrientos, J.C.; Zelenetz, A. D.; Kipps, T. J.; Flinn, I.; Ghia, P.; Eradat, H.; Ervin, T.; Lamanna, N.; Coiffier, B.; Pettitt, A. R.; Ma, S.; Stilgenbauer, S.; Cramer, P.; Aiello, M.; Johnson, D. M.; Miller, L. L.; Li, D.; Jahn, T. M.; Dansey, R.D.; Hallek, M.; O'Brien, S. M. Idelalisib and Rituximab in Relapsed Chronic Lymphocytic Leukemia. *N. Eng.J. Med.,* **2014**, 997–1007.

(17) Shin, Y.; Suchomel, J.; Cardozo,M.; Duquette, J.; He, X.; Henne, K.; Hu, Y. L.; Kelly, R. C.; McCarter, J.; McGee, L. R.; Medina, J. C.; Metz, D.; Miguel, T. S.; Mohn, M.; Tran, T.; Vissinga, C.; Wong, S.; Wannberg, S.; Whittington, D. A.; Whoriskey, J.; Yu, G.; Zalameda, L.; Xuxia Zhang, X.; Cushing T.D. Discovery, Optimization, and in Vivo Evaluation of Benzimidazole Derivatives AM-8508 and AM-9635 as Potent and Selective PI3Kδ Inhibitors. *J. Med. Chem.* **2016**, *59*, 431-447.

(18) Ritchie, T. J.; Macdonald, S. J. F.; Young, R. J.; Pickett, S. D. The impact of aromatic ring count on compound developability: further insights by examining carbo- and hetero-aromatic and -aliphatic ring types. *Drug Discov. Today* **2010**, *16*, 164-171.

(19) Zientek, M.; Stoner, C.; Ayscue,R.; Klug-McLeod, J.; Jiang, Y.; West, M.; Collins, C.; Ekins, S. Integrated in silico-in vitro strategy for addressing cytochrome P450 3A4 time-dependent inhibition*Chem. Res. Toxicol.* **2010,** *23,* 664–676.

(20) Veber, D. F.; Johnson, S. R.; Cheng, H. Y.; Smith, B. R.; Ward, K. W.; Kopple, K. D. Molecular properties that influence the oral bioavailability of drug candidates. *J. Med. Chem.* **2002**, *45*, 2615-2623.

(21) Lipinski, C. A.; Lombardo, F.; Dominy, B. W.; Feeny, P. J. Experimental and computational approaches to estimate solubility and permeability in drug discovery and development settings *Adv. Drug Deliv. Rev.* **1997**, *23*, 3-25.

(22) Wold, S.; Sjöström, M.; Eriksson, L. PLS-regression: a basic tool of chemometrics. *Chemom. Intel. Lab. Syst.* **2001**, *58*, 109-130.

(23) Abad-Zapatero, C. Ligand efficiency indices for effective drug discovery. *Expert Opin. Drug Discov.* **2007**, *2*, 469-488.

(24) Tanaka, D.; Tsuda, Y.; Shiyama, R.; Nishimura, T.; Chiyo, N.; Tominaga, Y.; Sawada, N.; Mimoto, T.; Kusunose, N. A practical use of ligand efficiency indices out of the fragment-based approach: ligand efficiency-guided lead identification of soluble epoxide hydrolase inhibitors. *J. Med. Chem*. **2011**, *54*, 851–857.

(25) Yamamoto, Y.; Arakawa, T.; Ogawa, R.; Itoh, K. Ruthenium(II)-Catalyzed Selective Intramolecular [2 + 2 + 2] Alkyne Cyclotrimerizations. *J. Am. Chem. Soc.* **2003**, *125*, 12143-12160.

(26) Trost, B.; Rudd, M. T.; Costa, M. G.; Lee, P. I.; Pomerantz, A. E. Regioselectivity control in a ruthenium-catalyzed cycloisomerization of diyne-ols. *Org. Lett*. **2004**, *6*, 4235-4238.

(27) Chris Tame PhD thesis, unpublished work.

(28) Erdik, E. Use of activation methods for organozinc reagents.*Tetrahedron* **1987**, *43*, 2203-2212.

(29) Deng, J. Z.; Paone, D. V.; Ginnetti, A. T.; Kurihara, H.; Dreher, S. D.; Weissman, S. A.; Stauffer, S. R.; Burgey, C. S. Copper-facilitated Suzuki reactions: application to 2-heterocyclic boronate. *Org. Lett.* **2009**, *11,* 345-347.

(30) All animal studies were ethically reviewed and carried out in accordance with Animals (Scientific Procedures) Act 1986 and the GSK Policy on the Care, Welfare and Treatment of Animals.

(31) Compound **3**: pIC_{50} <5.0 against a panel of kinases comprised of ASK1, Aurora A, Aurora B, BTK, CHKB, Choline Kinase α, DAG Kinase, DAG Kinase Zeta, EGFR (HER1), FRAP1, GSK3B, IKK1, IKK2, ITK, JAK2, JAK3, LCK, LRRK2, PI4K2A, PIK3C2B, PIK4A, PIL4B, PIP4K2A, ROCK1, SPHK1, SPHK2 and SYK; also pIC50 pIC_{50} <5.0 against p38a and PDE4B. DNA-PK apparent pIC50 = 5.6 and equivocal data were reported in assays related to VPS34 inhibition.

(32) Valko, K.; Nunhuck, S.; Bevan, C.; Abraham, M. H.; Reynolds, D.P. Fast gradient HPLC method to determine compounds binding to human serum albumin. Relationships with octanol/water and immobilized artificial membrane lipophilicity. *J. Pharm. Sci.,* **2003**, *92,* 2236-2248.

[33](33) Bhattachar, S. N.; Wesley, J. A.; Seadeek, C. Evaluation of the chemiluminescent nitrogen detector for solubility determinations to support drug discovery. *J. Pharm. Biomed. Anal.* **2006**, *41*, 152−157.